Sulcal Variability of Twins

Gabriele Lohmann, D. Yves von Cramon and Helmuth Steinmetz[1]

Max-Planck-Institute of Cognitive Neuroscience, Stephanstrasse 1a, 04103 Leipzig and [1]Klinik für Neurologie, J.W. Goethe-Universität Frankfurt am Main, Schleusenweg 2-16, 60590 Frankfurt, Germany

We investigated three-dimensional, depth-encoded line representations of neocortical sulci calculated from magnetic resonance image (MRI) datasets of 19 pairs of normal monozygotic twins. Monozygotic co-twins were significantly more alike than control pairs of unrelated twins matched from the same sample. Sulcal depth influenced sulcal similarity, with deeper sulci being more similar than superficial sulci. This was true both for the pairs of related co-twins and for the unrelated pairs, although the sulcal depth effect was stronger for the related twins. Our results indicate that the shape of deep (ontogenetically early) sulci of the human brain is more strongly predetermined than that of superficial sulci. The finding that sulcal similarity increased with sulcal depth especially within monozygotic twin pairs should stimulate further investigations of the relative importance of genetic versus shared environmental morphogenetic factors that must account for this result. In addition, we found that subjects with similar brain shape also have more similar sulcal patterns, suggesting that both features are the result of ontogenetically related processes. Sulcal comparisons across the entire sample suggested that the left posterior lateral hemispheric surface may be the least variable brain area. Methodologically, these results were obtained by the representation of sulci as three-dimensional polygonal lines (termed 'sulcal cuts') that are extracted automatically from MRI data sets using new image analysis techniques.

Introduction

Twin studies play an important role in our attempts to elucidate the unknown mechanisms of gyral/sulcal ontogenesis in humans [reviewed by Welker (Welker, 1990)].

Several groups have recently performed magnetic resonance (MR) morphometric studies of the neocortical surface in twins. Tramo *et al*. reported a genetic influence on the size of several cortical surface areas, with the left hemisphere being under a stronger genetic control than the right (Tramo *et al*., 1995). Bartley *et al*. compared brain volume and external sulcal pattern in monozygotic and dizygotic twins. They found a strong heritability of brain volume, but only minor heritability effects on sulcal variation (Bartley *et al*., 1997). Surprising discordances among monozygotic twins for sulcal shape or planum temporale asymmetry have also been described by Steinmetz *et al.* (Steinmetz *et al.*, 1995).

The present analysis of sulcal variation is based on the same sample (Steinmetz *et al.*, 1995). However, we tried to aim beyond previous studies by including sulcal depth in our analysis. Specifically, we hypothesized that deeper sulci may be less variable than superficial sulci because deeper sulci appear early during ontogenesis and may be more strongly predetermined (Welker, 1990).

Methodologically, our new target was achieved by the representation of sulci as three-dimensional polygonal lines (termed 'sulcal cuts') that capture location and depth characteristics. Sulcal cuts are extracted automatically from magnetic resonance data (MRI) data using new image analysis procedures (Lohmann, 1998a). This new method offers distinct advantages over earlier methods used by Bartley *et al*. (Bartley *et al*., 1997). Their method was based on renderings of the cortical surface and was therefore subject to illumination artifacts and geometrical distortions due to viewpoint dependency. Our method eliminates these problems by using entirely three-dimensional techniques. In addition, our method allows sulcal depth to be measured.

Since sulcal depth is encoded in each vertex of a sulcal cut, we were able to study the degree to which sulcal variability is correlated with sulcal depth. Of course, this also allowed us to address the question of a possible influence of sulcal depth on anatomical variation in general, independent of the twin problem.

Materials and Methods

The MRI Data

Our input data consisted of T_1-weighted MRI data of 19 pairs of monozygotic twins (38 persons) of which 16 pairs were female and 3 were male. In 9 pairs, both siblings were right-handed, in the remaining 10 pairs, the siblings had different handedness. Discordant handedness is not unusual in identical twins. In fact, a previous study (Ellis *et al.*, 1987) showed that 25% of all pairs of identical twins are discordant for handedness (Shimizu and Endo, 1983).

The twins were recruited through announcements in the Medical School of the University of Düsseldorf and through newspaper advertisements specifically calling for participation in a handedness study (Steinmetz *et al*., 1995). The 19 pairs used in the present study reported no birth complication, neurological or psychiatric illness, learning disability or failure in elementary school. No abnormalities were detected on their MR images. They ranged in age between 13 and 62 years with a median of 25.5 (average 30.84). The MRI data were acquired on a Siemens 1.5 T machine using a 22 min fast-low-angle-shot MR sequence covering the entire brain. The spatial resolution was 1 × 1 × 1.17 mm.

Our data analysis consisted of three major steps. Firstly, to account for differences in the overall brain shape and size we applied a brain shape normalization to each data set so that all brains were geometrically transformed into a single standard shape. Secondly, we applied a sequence of image analysis procedures to each data set in order to extract a line representation of the sulcal pattern. Thirdly, we performed pairwise comparisons on the sulcal lines using a similarity metric that was based on local proximity measurements. In the following, each of these steps will be described in greater detail.

Brain Shape Normalization

All data sets were initially subjected to a standard preprocessing routine which ensured that all data sets were rotated into a standard coordinate system whose origin was halfway between AC and CP (Fox *et al.*, 1985). At the same time, all data sets were resampled to a spatial resolution of 1 mm. In addition, we applied an automatic procedure to separate brain from non-brain material. For a more detailed description of our preprocessing procedure see Kruggel and Lohmann (Kruggel and Lohmann, 1997).

Human brains differ greatly in their overall shape and size. In order to eliminate the effect of shape differences all data sets must be subjected to

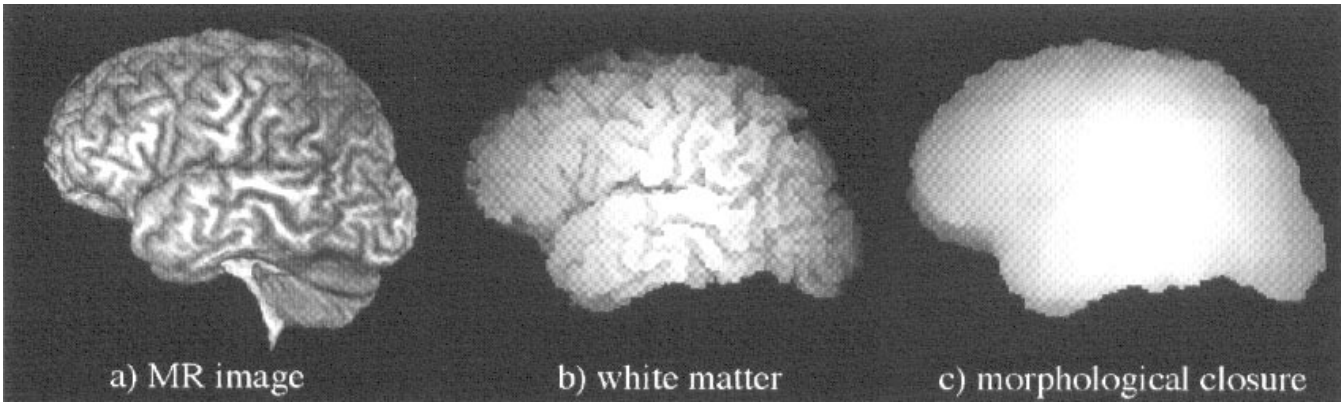

Figure 1. Definition of overall brain shape. (*a*) Original MR image; (*b*) the result of the white matter segmentation; (*c*) the morphological closure which defines the overall brain shape.

a shape normalization. Spatial normalization is frequently used in the context of human brain mapping in an effort to remove intersubject or intermodal variability (Fox, 1995; Friston *et al.*, 1995; Glass *et al.*, 1995; Maziotta *et al.*, 1995). Generally, the aim is to geometrically align one data set with another such that corresponding brain locations are mapped onto each other and spatial variability is diminished.

As in the present context our objective is to quantify the variability of the sulcal pattern, we only seek to remove intersubject variability in so far as it is caused by differences in the overall brain shape or size. Clearly, such a shape normalization must not make use of anatomical landmarks that are based on the sulcal pattern. Therefore, we employ a global and stationary transformation that minimizes the distance between overall brain shapes irrespective of the sulcal pattern.

A prerequisite for any normalization process is the definition of the overall brain shape and the definition of a standard shape. Clearly, a simple Talairach space normalization would be too crude in this context.

For the present study, the overall shape was defined by a sequence of image analysis procedures as illustrated in Figure 1. We begin with a white matter segmentation which separates white matter from other tissue classes using the algorithm described by Lohmann (Lohmann, 1997). At the same time, we automatically remove the cerebellum and the brain stem (Lohmann, 1998b) (Fig. 1*b*). The overall brain shape is defined as the three-dimensional morphological closure of the white matter (Maragos and Schafer, 1990) (Fig. 1*c*).

We computed the morphological closures of all 38 data sets. To normalize brain shapes, we selected a 'model' brain from these 38 data sets to which all other brains were subsequently deformed. We selected the model brain by computing pairwise discrepancies between all data sets, and choosing the one whose average discrepancy to all other brains was the least in this group.

All data sets were initially subjected to a linear scaling in the x, y and z directions so that they all had the same bounding box. To eliminate more subtle differences in brain shape, we additionally applied a non-linear deformation using third-order polynomials of the form:

$$f(x,y,z) = a_1x + a_2y + a_3z + a_4xy + a_5xz + a_6yz + a_7x^2 + a_8y^2 + a_9z^2 + a_{10}xyz + a_{11}x^2y + a_{12}x^2z + a_{13}y^2x + a_{14}y^2z + a_{15}z^2x + a_{16}z^2y + a_{17}x^3 + a_{18}y^3 + a_{19}z^3$$

The deformation parameters were $a_1, \ldots, a_{19}$ were estimated as follows. For each point p_i, $i = 1, \ldots, n$ on the surface of the morphological closure we selected a point q_i on the surface of the morphological closure of the model brain whose Euclidean distance from p_i was minimal. We then selected the parameters a_j, $j = 1, \ldots, 19$ such that the term

$$\sum_i^n \left[q_i - f(a_1,\ldots,a_{19};\, p_i)\right]^2$$

was minimized. To simplify the computation we did not use all the surface voxels. Instead, we chose a randomly selected set of points such that the points were approximately evenly distributed across the surface and the average distance between points was ~3 mm.

This process was applied to the x, y and z directions separately, so that for each data set 3 × 19 = 57 non-linear deformation parameters resulted.

To evaluate the quality of the normalization, we performed pairwise comparisons of brain shapes before and after normalization. For each pair of data, we measured the shape similarity using the term:

$$dist = \frac{1}{n}\sum_{i=1}^{n} \|p_i - q_i\|$$

where p_i and q_i are defined as before. The term *dist* represents the average distance in millimeters between corresponding points on the surface of the morphological closures. The discrepancy was measured across the lateral brain surface.

Table 1
The results of shape normalization

	Before normalization	After linear scaling	After non-linear scaling
Twins	3.129 (0.321)	3.183 (0.288)	2.687 (0.096)
Unrelated pairs	4.797 (1.189)	3.820 (0.479)	2.820 (0.074)
Relative error	0.53	0.20	0.05

The numbers denote average discrepancies between points on the surfaces of the morphological closures. SDs in parenthesis.

The results of the normalization process are shown in Table 1. The similarity values of the set of 19 co-twin pairs was contrasted with a set of 19 pairs of unrelated subjects taken from the same data pool ('unrelated pairs') which was obtained by reshuffling the twin pairs. Note that both sets consist of *pairs* of subjects, not of individual subjects.

The set of unrelated pairs was chosen to have similar gender and handedness characteristics as the set of twins. Note that twins have a higher degree of similarity in brain shape both before and after normalization. Using normalization, however, the average discrepancy between co-twin pairs and the unrelated pairs dropped from 4.797 to 3.129 = 1.668 to 0.133 mm. The relative error, which is defined as $(\mu_{twins} - \mu_{nontwins})/\mu_{twins}$ dropped from 0.53 to 0.05, where μ_X denotes the average of the sample X. The fact that the average discrepancy is still >2.6 mm is due to the fact that the surface points have an average distance of ~3 mm.

Extracting Line Representations of Sulcal Patterns

To facilitate intersubject comparisons of sulcal patterns, we apply a sequence of image analysis steps which reduces the input data to highly condensed line representations of the cortical folding which we call 'sulcal cuts' (Lohmann, 1998a). We define sulcal cuts to be line representations of sulci extracted at one specific level of depth ('cut' at that level). We define 'depth' as the distance towards an idealized smooth brain surface. Figure 2 illustrates the sequence of image analysis steps required to extract the sulcal cuts. The first few steps are identical to the

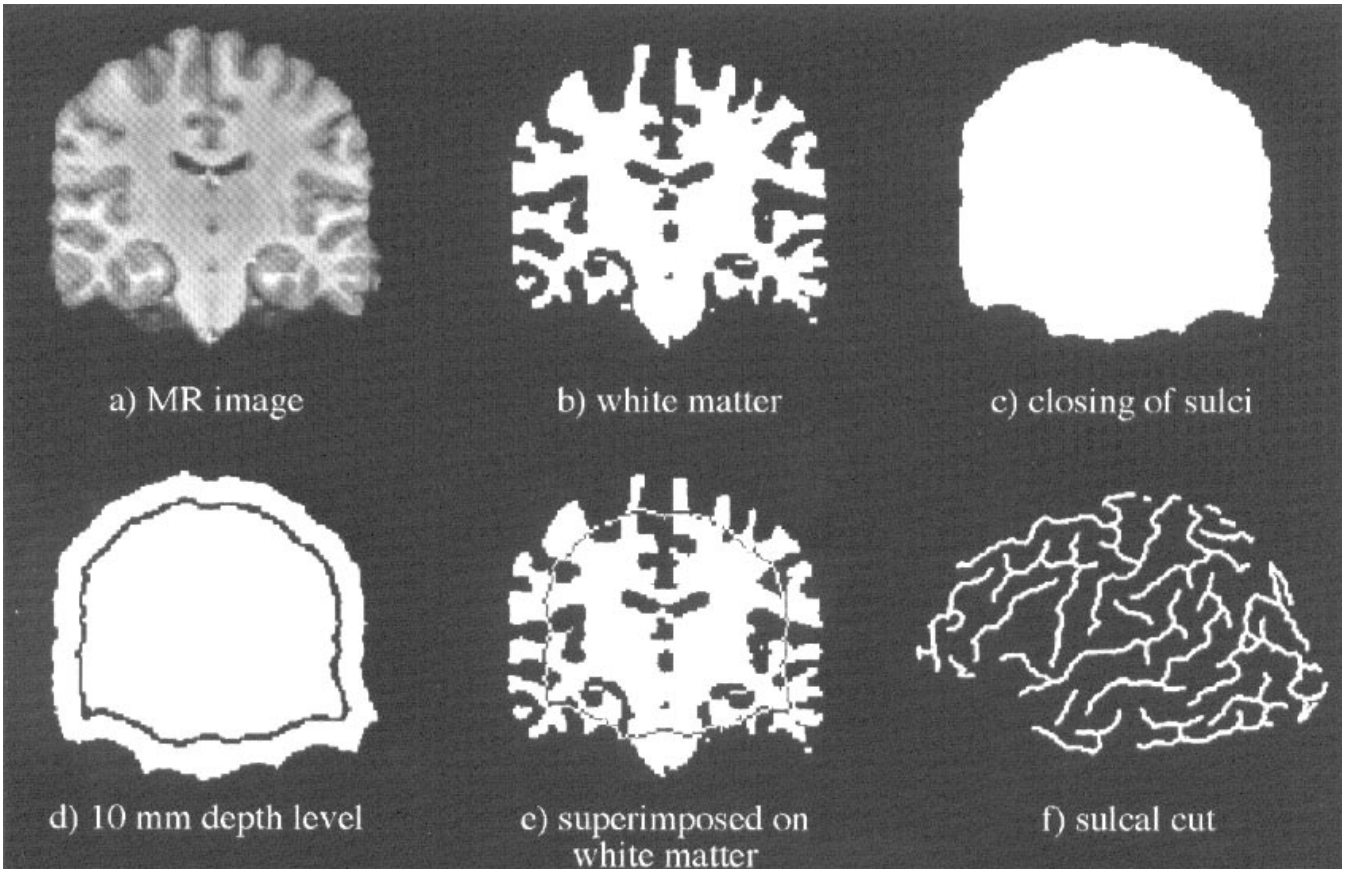

Figure 2. Image analysis steps for extracting sulcal cuts. For ease of presentation only one coronal slice is shown here, even though the procedure is entirely three-dimensional (Lohmann, 1998a).

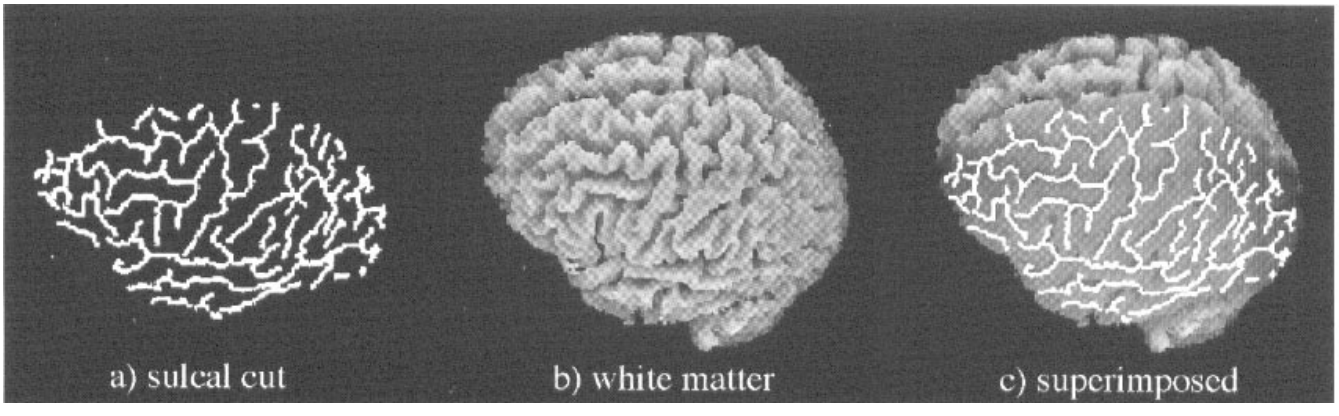

Figure 3. Sulcal cuts superimposed on white matter renderings viewed from top left (Lohmann, 1998a).

ones used for computing the morphological closure. Specifically, the input data set (Fig. 2*a*) is first subjected to a white matter segmentation (Fig. 2*b*) which separates white matter from other tissue classes. This step helps to make the sulcal indentations more pronounced and thus more easily identifiable. The white matter segmentation essentially 'decorti--cates' the brain by eroding the outer layers of cortex. It does however not clearly differentiate between white matter and subcortical structures.

We then close the sulci using a three-dimesnional morphological closing filter (Maragos and Schafer, 1990) (Fig. 2*c*) to obtain an idealized smoothed surface. The depth level is computed with respect to this surface using a three-dimensional distance transform (Borgefors, 1984). Figure 2*d* shows a depth level of 10 mm, which is shown superimposed on the white matter in Figure 2*e*.

We then apply a three-dimensional topological thinning procedure (Tsao, 1981; Lohmann., 1998a) which reduces the sulcal interiors to thin skeletal medial surfaces positioned in the center of the sulcus. The intersection of medial surfaces with the depth level yields the sulcal cuts. For the present study, we only investigated the lateral sulci. The basal sulci, the Sylvian fissure and the interhemispheric cleft were removed. Figure 2*f* shows the result as a three-dimensional rendering viewed from the left.

The correctness of the line extraction process can be assessed by

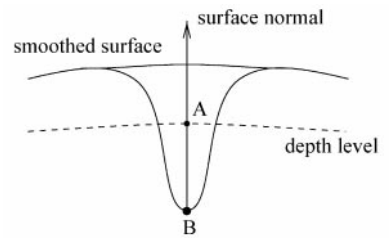

Figure 4. Depth-labeling of sulcal cuts.

superimposing a three-dimensional rendering of the white matter with the three-dimensional rendering of the sulcal cut as shown in Figure 3 (Lohmann, 1998a).

Depth Estimation

At this stage of the procedure, the input image is reduced to a set of lines of voxels representing a depth level cut through the sulcal pattern at one predefined depth level. We now estimate the depth of the sulcal valley 'underneath' each such point as follows (see Fig. 4).

Let A denote the sulcal point to be labeled. We compute the normal to the depth level at A and follow the direction opposite to the normal direction until we hit the sulcal bottom. The point where the inverse normal intersects the bottom is marked as B in Figure 4. From the distance transform that was applied in a previous step, each point – including point B – has already been given a depth label denoting its distance to the smoothed out idealized surface (see Fig. 2*c*,*d*). We now attach B's depth level to point A. This procedure is applied to every point in the sulcal depth cut.

Using the above algorithm, we obtained depth-labelled sulcal cuts at the 5 mm depth level for each of our 38 data sets. Figure 5*a*,*b* shows depth-encoded sulcal cuts of two pairs of twins from our data pool in a color-coded rendering, where red represents deep sulcal parts and blue represents shallow parts.

Definition of the Similarity Metric

Once sulcal cuts have been identified and geometrically transformed to a standard brain shape, pairwise comparisons of sulcal cuts using local proximity measurements can be performed.

The degree of similarity between two sulcal cuts is defined as follows. Let u denote the first set of sulcal lines, and v the second set of sulcal lines. For each point p_i, $i = 1, \ldots, m$ of u we select a point q_i of v such that the Euclidean distance $|q_i - p_i|$ is minimal. The points (q_i, p_i) are said to 'match' if this distance is less than some predefined threshold. In our experiments, we used a threshold of 2.5 mm. The exact choice of the threshold is not critical as will be shown in the next section.

The degree of similarity $t(u,v)$ between the two sulcal cuts u,v is then defined as the percentage of the points in u that had a match in v. More precisely, let $n(u)$ denote the total number of sulcal points in u, and $m(u,v)$ denote the number of points in u that have a match in v; then

$$t(u,v) = \frac{m(u,v)}{n(u)}$$

Note that this measure is not symmetrical as the number of points may vary across sets of sulcal lines, so that usually $t(u,v) \neq t(v,u)$. Therefore, we redefine our similarity measure as

$$s(u,v) = 0.5\left[t(u,v) + t(v,u)\right]$$

In order to investigate the influence of depth on the degree of similarity, the above metric can be constrained to specific levels of depth as follows. Remember that each point p_i, $i = 1, \ldots, m$ of the set of sulcal lines has a depth label d indicating the depth of the sulcus 'underneath' this point.

Two points (q_i, p_i) from two sulcal cuts u,v are said to match at depth $[d_a, d_b]$ if their distance $|q_i - p_i|$ is minimal, and

$$d_a \leq depth(p_i) \leq depth(q_i) \leq d_b$$

In this case, let $n(d_a,d_b;\ u)$ denote the number of sulcal points in u between depth levels d_a and d_b, and let $m(d_a,d_b;\ u,v)$ be the number of points that have a match at that depth in v, then the constrained similarity between u,v is defined as:

$$t(d_a,d_b;u,v) = m(d_a,d_b;u,v) / n(d_a,d_b;u)$$

and

$$s(d_a,d_b;u,v) = 0.5\left[t(d_a,d_b;u,v) + t(d_a,d_b;v,u)\right]$$

Figure 6 shows the sulcal cuts of a pair of twins. Points that match are shown in color.

Note that it is essential to take all similarity measurements at a single depth level cut, which in our case was set to 5 mm. To see why, imagine some pattern that is painted on the surface of some ellipsoid such as the sulcal pattern on a brain surface. If the ellipsoid is allowed to shrink, then the distances between any arbitrary points belonging to the pattern will decrease. Therefore, proximity measurements taken at cuts of different depth levels would have a depth-related bias.

Results

In our first set of experiments, we compared the set of 19 pairs of monozygotic co-twins against a reshuffled set of 19 pairs of unrelated twins ('unrelated pairs') taken from the same data pool, i.e. we 'reshuffled' the twin set so we got pairs of unrelated twins. For simplicity, we will sometimes refer to this set as the 'reshuffled set'. Note that both the twin set and the reshuffled set consist of *pairs* of subjects rather than of individual subjects.

The set of unrelated pairs was chosen such that it had similar gender and handedness characteristics as the set of co-twins. In particular, all pairs of the reshuffled set were made up of members of the same sex, and as in the twin set 16 pairs were females and 3 pairs were males. It contained 9 pairs of right-handers, 10 pairs were mixed right/left-handers. Each subject was used exactly once for the set of unrelated pairs.

The matching metric was evaluated for matches at three levels of depth called A, B and C, which were defined as follows. For each set of sulcal lines, we computed two depth thresholds T_a, T_b such that the set A contained points with shallow depth labels ranging from $[0, T_a]$, set B contains points of intermediate depth ranging from $[T_a, T_b]$ and set C contains the deepest points with labels in $[T_b, \infty]$. The three sets were chosen such that each contained approximately one-third of the total number of points. Thus, effects due to interindividual differences in sulcal depth were eliminated. All measurements were made using depth-labelled sulcal lines which were cut at a constant depth level of 5 mm.

Figure 7*a* shows the results for both the twin set and the reshuffled set. Note that the twin set had higher similarity values at all levels of depth. Figure 7*b* shows the difference in similarity between the two sets. Note that it increases with depth.

We performed both a two-tailed *t*-test and an analysis of variance to estimate the statistical significance of these results.

A *t*-test was used to estimate the statistical significance of the difference plot using the following approach. Let μ_A, μ_B and μ_C denote the average similarity values of the twin set at depth levels A, B and C, and let $\overline{\mu}_A$, $\overline{\mu}_B$ and $\overline{\mu}_C$ denote the average similarity values of the reshuffled set at A, B and C. We then tested whether $\mu_B - \mu_A$ is significantly larger than $\overline{\mu}_B - \overline{\mu}_A$. Likewise, we tested $\mu_C - \mu_B$ against $\overline{\mu}_C - \overline{\mu}_B$, and $\mu_C - \mu_A$ against $\overline{\mu}_C - \overline{\mu}_A$. The results are summarized in Table 2. Note that the increase in difference from B to C is significant ($P = 0.027$), and also from A to C ($P = 0.001$), but not from A to B.

An analysis of variance supports these results. We contrasted

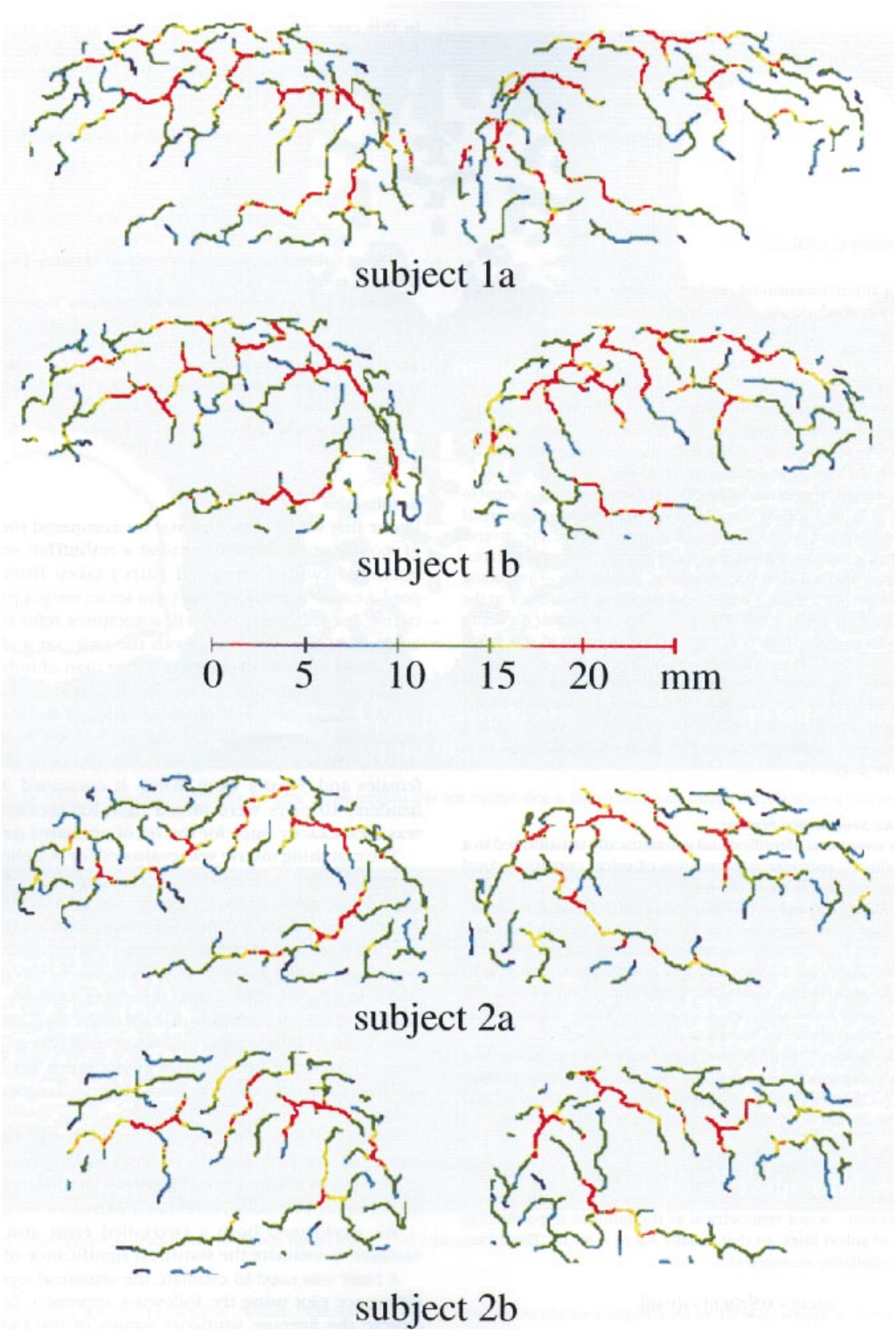

Figure 5. Depth-encoded sulcal cuts of two twin pairs.

the factor 'pair-relationship' with the factor 'depth'. The 'pair-relationship' had the two levels 'co-twin pair' versus 'unrelated pair', and the depth factor had the two levels 'A' versus 'C'. The results are shown in Table 3. Note that both depth and the pair-relationship strongly influence similarity. The interaction between depth and the twin-relationship is also statistically significant.

As noted in the previous section, we performed these tests with a fixed threshold of 2.5 mm in which we searched for matching points. To ascertain that the choice of the threshold is

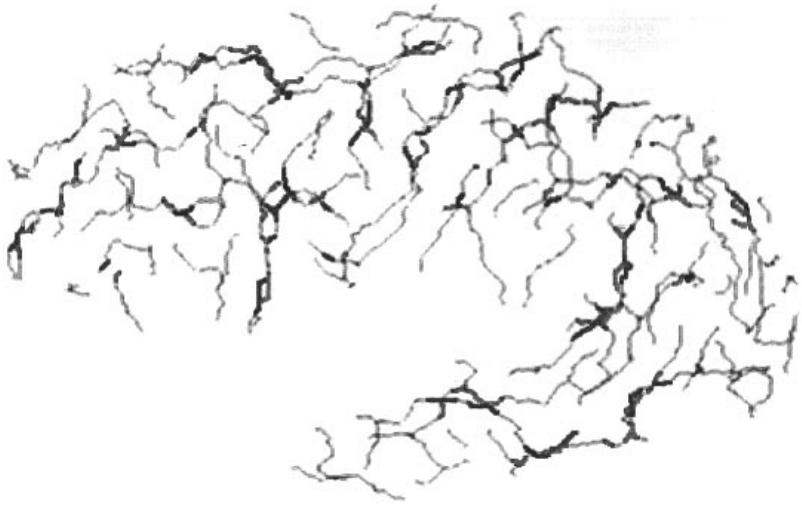

Figure 6. Sulcal cuts of twins, matching points are shown in black.

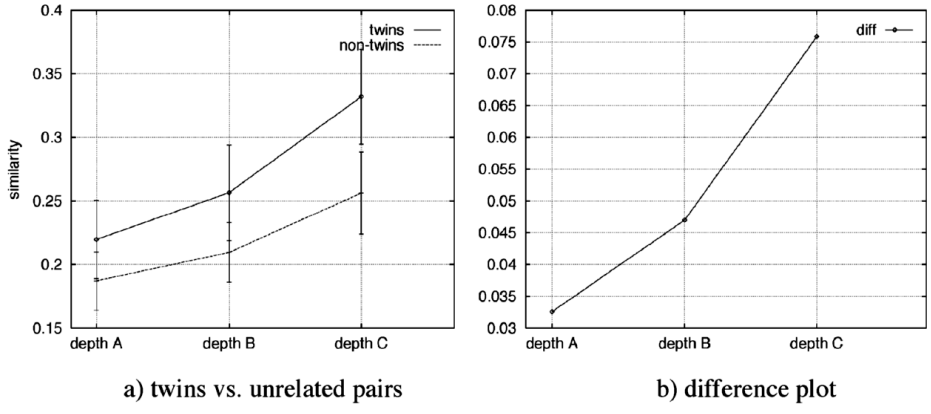

Figure 7. Similarity measurements. (*a*) Similarity values for the twin set and the set of unrelated pairs. (*b*) The difference in similarity between the two sets. Note the increase in difference with depth.

Table 2
Test of significance for the increase in difference

Depth	$\mu_X - \mu_Z$	$\overline{\mu}_X - \overline{\mu}_Z$	*P*-value
A to B	0.037 (0.040)	0.022 (0.035)	0.247
B to C	0.076 (0.038)	0.047 (0.039)	0.027
A to C	0.112 (0.036)	0.069 (0.040)	0.001

SDs in parenthesis.

Table 3
Analysis of variance

	F-value	*df*	*P*
Factor depth	215.63	1, 36	<0.001
factor pair	45.57	1, 36	<0.001
pair × depth	12.27	1, 36	0.0012

not critical we repeated the above tests with a larger threshold of 4.0 mm. Even though the percentage of matches increases in both sets, the relative discrepancies between the set of twins and the set of unrelated pairs remain approximately the same.

More precisely, at level A, the similarities for co-twins and the unrelated pairs were 0.410 and 0.366, respectively. They increased to 0.460 and 0.411 at level B, and finally to 0.541 and 0.462 at level C. The discrepancy between the two sets increased from 0.410 – 0.366 = 0.044 to 0.541 – 0.462 = 0.080. Thus, as for the smaller threshold, the discrepancy almost doubles from level A to level C. The statistical significance also remains intact.

In a second experiment, we investigated the effect of handedness on similarity. We contrasted a set of eight concordant right-handed female twins against eight pairs of unrelated female right-handers of the same data pool. We then performed the same experiment using eight female twins of discordant handedness who were contrasted with a control set of eight unrelated female pairs who were also discordant in handedness. Figure 8 shows the difference plots for these two experiments. The differences between these two sets was not significant.

Finally, we tested frontal versus posterior brain regions in both hemispheres. The frontal region was defined as all lateral sulci that are anterior with respect to the central sulcus, and the posterior region was defined as all remaining lateral sulci not including the central sulcus.

In the frontal region, the difference between the twin set and the reshuffled set is approximately the same for both the left and

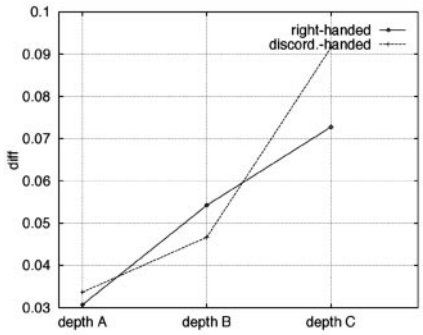

Figure 8. Difference plots for right-handed pairs and discordantly handed pairs.

the right hemisphere. However, at depth C the left posterior region of the unrelated pairs is significantly less different from the twin set than the right ($P = 0.561$).

Interpersonal Variability

Our definition of 'pairwise similarity', which is given by pairwise proximity measurements of sulcal cuts, naturally leads to a general definition of 'interpersonal variability' of an arbitrary population of subjects that is not restricted to the twin paradigm.

We define the degree of invariability in the sulcal pattern as the average pairwise similarities of pairs of subjects taken from a given population, where these pairs must be representative with respect to both gender and handedness. We measured sulcal variability in various brain regions both within the twin-pair set and the set of unrelated pairs

The following brain regions were tested: the frontal sulci (all sulci anterior with respect to the central sulcus, not including the central sulcus) with the posterior sulci (all remaining sulci, not including the central sulcus), and the central sulcus (CS). Table 4 shows the average pairwise similarities for each brain region.

The above significance levels were corroborated by a non-parametric Wilcoxon rank sum test. Note that interhemispheric differences in variability are much more pronounced in the posterior sulci than in the frontal regions, with the left having a significantly lower degree of variability.

All of the above values are given only for the deepest depth level C. At levels A and B we did not find any significant interhemispheric differences in variability. However, for most of the above subsets we found a highly significant decrease in variability from the most shallow depth level A to the deepest level C. Table 5 lists the *P*-values for the decrease in variability from level A to level C.

Brain Shape and the Sulcal Pattern

We found a significant correlation between similarities in the sulcal pattern and similarities in brain shape which became apparent through the following experiments.

We performed pairwise similarity measurements for both brain shape and sulcal patterns in both the set of twin pairs and the set of unrelated pairs. The similarity metric used for measuring brain shapes was the same as the one introduced before which gives the average discrepancy between closest points. All brains were first scaled linearly to a standard size so they had the same extent in all three dimensions. We did not apply a non-linear registration as we wanted to keep the general brain shape intact.

Table 4
Average pairwise similarities (pairs of co-twins, unrelated pairs)

	Twins	Unrelated pairs
Left hemisphere	0.327 (0.06)	0.263 (0.05)
Right hemisphere	0.336 (0.05)	0.247 (0.04)
Difference	NS	NS
Left frontal	0.318 (0.10)	0.261 (0.07)
Right frontal	0.311 (0.08)	0.280 (0.09)
Difference	NS	NS
Left CS	0.381 (0.15)	0.220 (0.14)
Right CS	0.397 (0.18)	0.221 (0.17)
Difference	NS	NS
Left posterior	0.329 (0.08)	0.276 (0.06)
Right posterior	0.336 (0.07)	0.223 (0.07)
Difference	NS	L ($P = 0.017$)

The symbol 'L' means that the average similarity values in left hemispheres were significantly higher than those of the right with values of a two-tailed *t*-test <0.05. NS, indicates that no significant difference between left and right hemispheres was found ($P > 0.10$). SDs in parenthesis.

Table 5
P-values for the decrease in variability from depth level A to depth level C

	Twins	Unrelated pairs
Left hemisphere	<0.001	<0.001
Right hemisphere	<0.001	<0.001
Left frontal	<0.001	<0.001
Right frontal	0.003	0.002
Left posterior	<0.001	<0.001
Right posterior	0.011	0.012

For the sulcal pattern we used our standard similarity metric. Those measurements were taken for the deepest 50% of sulcal points (level V) and for the 50% most shallow points (level U), as well as for all points of all depths (level U + V). Measurements of brain shape do not depend on depth, of course. Table 6 shows the mean discrepancy in brain shapes, the mean similarities of the sulcal pattern and Pearson's correlation coefficients for both sets. Note that in the reshuffled set there exists a clear inverse correlation ($r = -0.707$) between discrepancies in brain shapes and similarities in the sulcal pattern. The twin population shows roughly the same tendency which is however less significant.

Probabilistic Maps

Finally, we compiled a map which displays the probability of the occurrence of a match between twin siblings for each location in the standardized coordinate system. This map was produced as follows. For each data set, we marked all points which had a match in the corresponding twin data set where matches were constrained to the depth interval of 10–35 mm. We then assembled all marked points from all 38 data sets into a single combined data set. For each location, we counted the number of data sets from which a marked point was present within a search radius of 3.5 mm. To estimate probability we scaled these counts so that a value of x at one location means that within a radius of 3.5 mm marked points from x percent of all data sets were present.

Figure 10*a* shows local maxima of this map superimposed onto the sulcal lines of one individual subject. Locations at which >35% of the subjects had matches in their sulcal lines are shown as coloured blobs. The highest probabilities (shown in

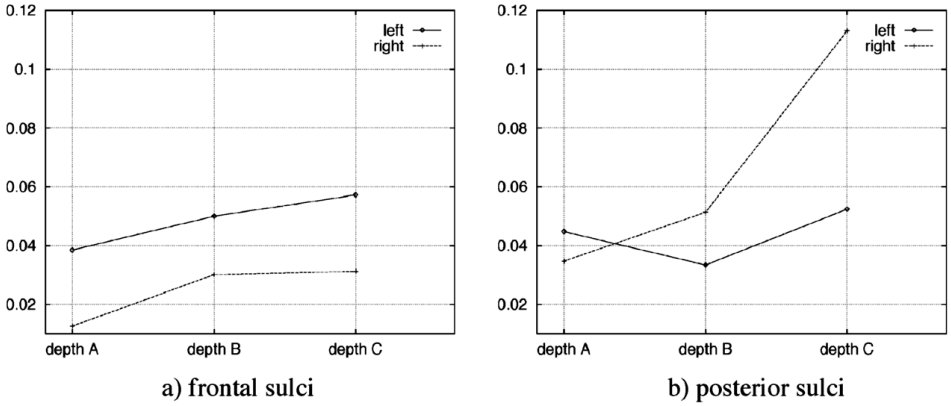

Figure 9. Difference plots for brain regions, left versus right hemispheres. (*a*) Shows differences between co-twins and unrelated pairs in both the left and right hemispheres of the frontal sulci. (*b*) The corresponding results for posterior sulci.

Table 6
Correlation between brain shape and sulcal pattern

	Brain shape	Sulcal pattern	Correlation	*P*-value
Twins				
Level U	3.183 (0.068)	0.265 (0.007)	–0.077	0.753
Level V	3.183 (0.068)	0.383 (0.009)	–0.444	0.057
Level U+V	3.183 (0.068)	0.453 (0.011)	–0.359	0.131
Unrelated pairs				
Level U	3.820 (0.113)	0.232 (0.007)	–0.611	0.005
Level V	3.820 (0.113)	0.312 (0.007)	–0.460	0.047
Level U+V	3.820 (0.113)	0.395 (0.007)	–0.707	0.001

SDs in parenthesis.

red) are reached in the left intraparietal sulcus with values >70%. Values >60% are attained in the left central sulcus and the left superior temporal sulcus.

Similarly, we produced a map in which matches between unrelated pairs of subjects are highlighted (Fig. 10*b*). Both maps are significantly correlated, with Pearson's correlation coefficient $r = 0.696$ ($P < 0.0001$).

General Discussion

Discussion of Methodological Aspects

In this paper we have introduced a new method for describing the human cortical topography. The sulcal pattern is represented by polygonal lines called 'sulcal cuts' which are extracted at a given depth. Each point belonging to a sulcal cut is given a label that indicates the depth of the sulcus underneath. Thus, sulcal cuts capture position, shape and depth characteristics of sulci. Unlike the method used by Bartley *et al.* (Bartley *et al.*, 1997) our method is entirely three-dimensional and is therefore not subject to viewpoint dependency or illumination artifacts.

The accuracy of the results of the line extraction method can be visually assessed by comparing the three-dimensional renderings of the white matter and of the sulcal lines. This procedure does not permit a quantitative evaluation of errors, but it does provide a means of visually verifying the results. For a more detailed discussion of the line extraction procedure and its verification see Lohmann (Lohmann, 1998a).

Line representations are an alternative to surface representations as used, for instance, by Tramo *et al.* (Tramo *et al.*, 1995). Such representations capture different aspects of the cortical topography, such as shape and position of sulci, which are not explicitly available in surface representations. At the same time, we arrive at a new definition of sulcal variability which measures variations in shape and position of sulci rather than variations of surface size. Both aspects are of course related: a highly convoluted and deep sulcus generates greater surface size.

Sulcal variability has been investigated in a number of related works. Evans *et al.* constructed a probabilistic atlas in Talairach space, where variability can be assessed by the sharpness of the gray level contours (Evans *et al.*, 1996). Thompson *et al.*, for instance, describe variability of sulcal surfaces in terms of displacement fields (Thompson *et al.*, 1996). Hill *et al.* use active shape models to describe variations of three-dimensional shapes in medical images (Hill *et al.*, 1993).

Our definition of sulcal variability differs from these and others in that it does not try to solve the correspondence problem. We do not seek to deform the sulcal pattern of one data set into that of another. Instead, we compute the average pairwise discrepancies of sulcal patterns by counting the number of close matches between points on sulcal lines. These matching points however, are not necessarily corresponding points in a strictly neuroanatomical sense. Rather, we view variability in terms of pairwise discrepancies between any two sets of scattered and unstructured points.

This approach greatly simplifies the problem of measuring variability. Its disadvantage is that it does not solve the correspondence problem. Its advantage is its simplicity and reliability.

The metric we used for measuring the discrepancy between such point sets is quite straightforward. It counts the number of sulcal points that are present from both data sets within a small search radius. We have shown that the size of the search radius is not critical: enlarging it does not significantly alter the results. However, if the radius becomes too large, then points from entirely different sulci may enter the same search radius so that the results become unreliable and the discriminative power is lost. Since our standard radius was very small (2.5 mm) this type of error was unlikely to occur.

An alternative metric that is sometimes used for comparing biological shapes represented by point sets is the Procrustes metric (Bookstein, 1991), which is approximately equal to the square root of the sum of squared differences between positions of landmark data. However, it is only applicable if correspondences between landmarks are known. Finding corresponding points along sulcal cuts is extremely difficult and unreliable. Furthermore, not every point along a sulcal cut is guaranteed to have a uniquely identifiable matching point in the

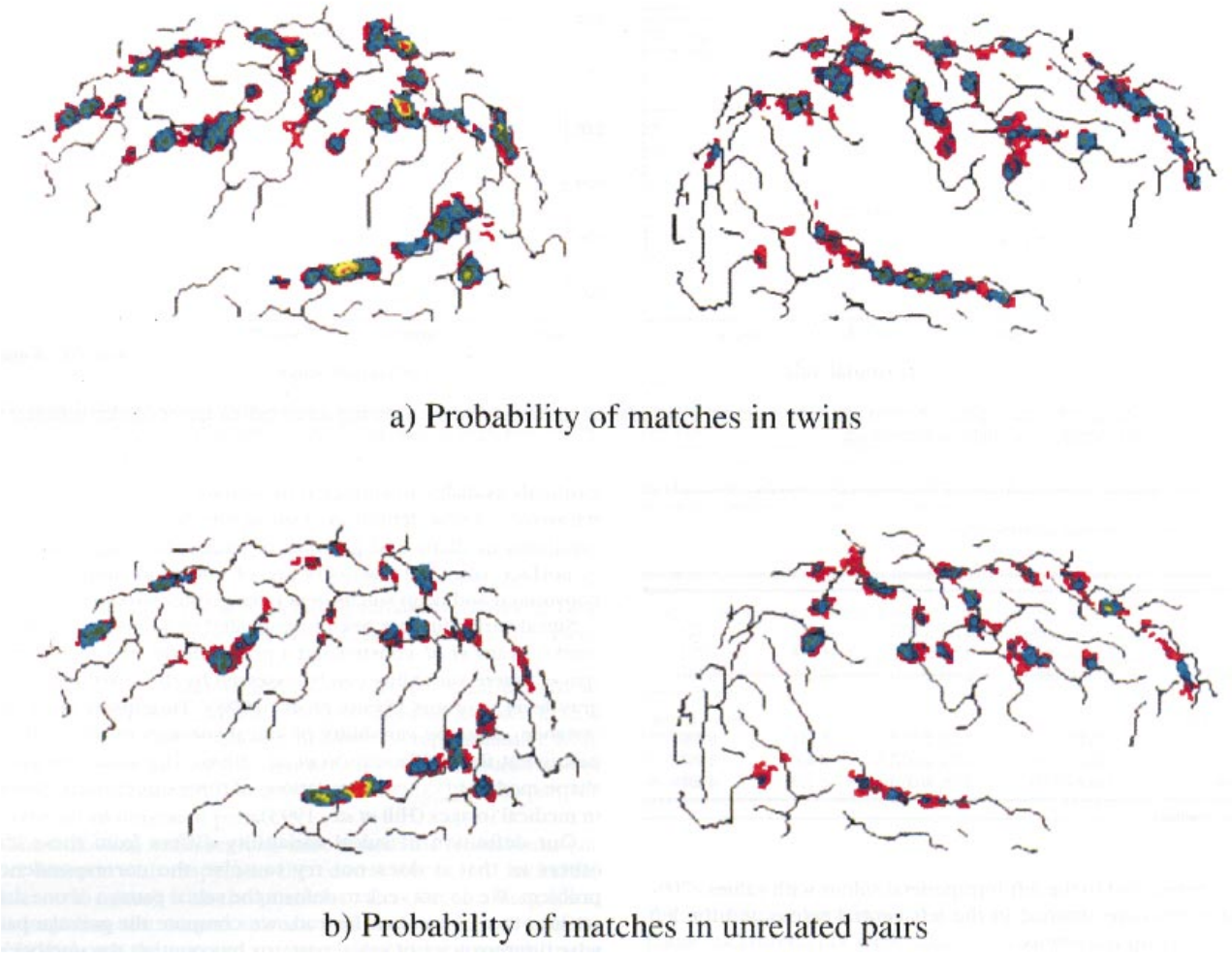

Figure 10. Probability maps. Probability of matches in twins (*a*) and unrelated pairs (*b*).

other data set. For those reasons we chose not to use Procrustes distances for this task. Another distance metric that is often used for comparing sets of points is the Hausdorff distance (Edgar, 1995). However, it is much too crude in our context and extremely sensitive to outliers.

Brain shape normalization plays a crucial role in determining discrepancies between sulcal patterns. We used a type of shape normalization that is not based on any cortical landmarks as we wanted to distinguish between discrepancies of brain shape and sulcal pattern. Had we used cortical landmarks for normalization these two types of discrepancies would have interfered and thus have invalidated our results.

Unfortunately, as can be seen from Table 1, the method we use for shape normalization has not quite eliminated all discrepancies between shapes. Brain shapes of twins are still more similar even after normalization than those of unrelated pairs of subjects. However, shape normalization affects all levels of sulcal depth to the same degree, and therefore the results related to sulcal depth cannot be attributed to shape normalization problems.

Discussion of Results

Our three-dimensional analyses of the human sulcal pattern have shown that monozygotic twins are significantly more alike than unrelated twin subjects. This finding is not surprising and agrees with the MRI study of Bartley and co-workers, who recently reported that the heritability of the gyral pattern may range between 7 and 17% (Bartley *et al.*, 1997). In contrast to their study population, ours did not include dizygotic twins, so that we cannot calculate similar heritability estimates for our anatomical data. A new finding of the present study, however, is the interaction of sulcal depth with the degree of similarity between subjects, particularly within monozygotic twin-pairs. Both the anatomical similarity of related co-twins and of unrelated twins increased with sulcal depth as determined by *t*-tests and analyses of variance. The difference in similarity between pairs of related versus unrelated twins increased with sulcal depth, the related twins becoming more alike than the unrelated pairs.

These findings suggest that the shaping of deeper sulci is more strongly predetermined than that of superficial ones. This main result of our study is likely to reflect the timing of gyral ontogenesis, where the deep sulci are the first to appear, followed by the more shallow ones. The younger the sulcus, the stronger appears to be the influence of (non-genetic) factors leading to sulcal variation. Considering these findings in relation to the concept of 'gyrogenesis' (farther outward movement of gyral crowns compared to sulcal fundi during brain development), we

speculate that the ontogenetic 'proto-map' of sulcal fundi generally looks more alike than the superficial sulcal pattern, not only among twins.

Most sulci and gyri of the human brain develop in the last gestational trimester and are visible at birth (Retzius, 1896; Chi *et al.*, 1977). Nevertheless, the brain still almost triples its size between birth and adulthood, and cortical folding (i.e. sulcal deepening) continues throughout this period (Armstrong *et al.*, 1995).

Cytoarchitectonic differentiation, ongoing ingrowth of thalamic afferents, selective neuronal death and progressive myelination are among the 'micromechanic forces' that probably influence ongoing gyrification (Welker, 1990). It is plausible to assume that such factors can be modified in large part by non-genetic influences, such as use-dependent functional activity (Rakic, 1988).

Our analyses of sulcal variability related to gender, handedness and various brain regions showed that the left posterior region was significantly less variable in right-handers than the right posterior. We found no significant difference in variability between the left frontal and right frontal brain. Tramo *et al.* have previously reported a lower degree of variability in surface size for the left hemisphere (Tramo *et al.*, 1995); this is now confirmed by our results even though our notion of variability is quite different. For all brain regions we found that the deepest sulci are less variable than the shallowest ones. Overall brain shape appears to play an important role in determining sulcal shapes as suggested by the high inverse correlation between pairwise brain shape discrepancy and sulcal similarity. The fact that both brain shapes and sulcal patterns of twins are highly similar may perhaps also be viewed in this light. If indeed sulcal shapes are influenced by the overall brain shape, then shape normalization can be instrumental in reducing interindividual sulcal variability.

Notes

The authors would like to thank Dr. F. Kruggel for his help in the preprocessing of the MRI data. Supported by the Deutsche Forschungsgemeinschaft, SFB 194/A14.

Address correspondence to Gabriele Lohmann, Max-Planck-Institute of Cognitive Neuroscience, Stephanstrasse 1a, 04103 Leipzig, Germany.

References

Armstrong E, Schleicher H, Omran H, Curtis M, Zilles K (1995) The ontogeny of human gyrification. Cereb Cortex 5:56–63.

Bartley AJ, Jones DW, Weinberger DR (1997) Genetic variability of human brain size and cortical gyral patterns. Brain 120:257–269.

Bookstein FL (1991) Morphometric tools for landmark data. Cambridge: Cambridge University Press.

Borgefors G (1984) Distance transforms in arbitrary dimensions. Comput Vis Graphics Image Process 27:321–345.

Chi JG, Dooling EC, Gilles FH (1977) Gyral development of the human brain. Ann Neurol 1:86–93.

Edgar GA (1995) Measure, topology, and fractal geometry, 3rd edn. Berlin: Springer-Verlag.

Ellis SJ, Ellis PJ, Marshall E (1987) Hand preference in a normal population. Cortex 157–163.

Evans A, Collins DL, Holmes CJ (1996) Computational approaches to quantifying human neuroanatomical variability. In: Human brain mapping: the methods (Toga AW, Maziotta JC, eds), pp. 343–361. San Diego: Academic Press.

Friston KJ, Ashburner J, Frith CD, Poline JB, Heather JD, Frackowiak RSJ (1995) Spatial registration and normalization of images. Hum Brain Map 2:165–189.

Fox PT, Perlmutter JS, Raichle ME (1985) A stereotactic method of anatomical localization for positron emission tomography. J Comput Assist Tomogr 9:141–153.

Fox PT (1995) Spatial normalization origins: objectives, applications, and alternatives. Hum Brain Map 3:161–164.

Glass TG, Lankipalli BR, Downs H, Mayberg H, Fox PT, Lancaster JL (1995) A modality-independent approach to spatial normalization of tomographic images of the human brain. Hum Brain Map 3:209–223.

Hill A, Thornham A, Taylor CJ (1993) Model-based interpretation of 3D medical images. Fourth British Machine Vision Conference, pp. 339–348.

Kruggel F, Lohmann G (1997) Automatical adaptation of the stereotactical coordinate system in brain MRI data sets. IPMI 97 (Int. Conf. Information Processing in Medical Imaging), Poultney, VT.

Lohmann G (1997) A new approach to segmenting white matter from magnetic resonance images of the human brain. Technical Report, MPI, Leipzig.

Lohmann G (1998a) Extracting line representations of sulcal and gyral patterns in MR images of the human brain. IEEE Transactions on Medical Imaging, 17, 6:1040–1048.

Lohmann G (1998b) Automatic extraction of the cerebellum and the brain stem from MRI images of the human brain. Technical Report, Max-Planck-Institute of Cognitive Neuroscience, Leipzig, Germany.

Maragos P, Schafer RW (1990) Morphological systems for multidimensional signal processing. Proc IEEE 78:690–709.

Maziotta JC, Toga AW, Evans A, Fox P, Lancaster J (1995) A probabilistic atlas of the human brain: theory and rationale for its development. NeuroImage 2:89–101.

Rakic P (1998) Specification of cerebral cortical areas. Science 241: 170–176.

Retzius G (1896) Das Menschenhirn, Vols 1 and 2, Norstedt Soner.

Shimizu A, Endo M (1983) Comparison of patterns of handedness between twins and singletons in Japan. Cortex 19:345–352.

Steinmetz H, Herzog A, Schlaug G, Huang Y, Jäncke L (1995) Brain (a)symmetry in monozygotic twins. Cereb Cortex 5:296–300.

Thompson PM, Schwarz C, Lin RT, Khan AA, Toga AW (1996) Three-dimensional analysis of sulcal variability in the human brain. J Neurosci 16:4261–4274.

Tramo MJ, Loftus WC, Thomas CE, Gazzaniga M.S (1995) Surface area of human cerebral cortex and its gross morphological subdivisions: *in vivo* measurements in monozygotic twins suggest differential hemisphere effects of genetic factors. J Cogn Neurosci 7:292–301.

Tsao YF, Fu KS (1981) A parallel thinning algorithm for 3D pictures. Comput Graphics Image Process 17:315–331.

Welker W (1990) Why does cerebral cortex fissure and fold? A review of determinants of gyri and sulci. In: Cerebral cortex (Jones EG, Peters A, eds), Vol. 8b, pp. 3–136. New York: Plenum Press.